Applied Thermal Engineering 51 (2013) 1047–1054

Contents lists available at SciVerse ScienceDirect

Applied Thermal Engineering

journal homepage: www.elsevier.com/locate/apthermeng

Convective heat transfer and pressure drop characteristics of near-critical-pressure hydrocarbon fuel in a minichannel

Zhaohui Liu, Qincheng Bi*, Yong Guo, Jianguo Yan, Zhuqiang Yang

State Key Laboratory of Multiphase Flow in Power Engineering, Xi'an Jiaotong University, Xianning West Road #28, Xi'an 710049, China

HIGHLIGHTS

- Heat transfer coefficients can be predicted by Gnielinski correlation at $Re > 4000$.
- Adiabatic friction factors well agree with Moody diagram and Blasius correlation.
- Peak and trough exist in heat transfer coefficients near pseudo-critical points.
- Heat transfer deteriorated, together with instability and pressure drop deduction.
- At higher pressure, the singularity of heat transfer and fluid flow disappeared.

ARTICLE INFO

Article history:
Received 5 June 2012
Accepted 22 October 2012
Available online 30 October 2012

Keywords:
Heat transfer
Hydrocarbon fuel
Pressure drop
Pseudo-critical
Dynamic instability

ABSTRACT

The convective heat transfer and pressure drop characteristics of a kerosene kind hydrocarbon fuel were experimentally investigated in an electrically heated minichannel with an inside diameter of 2.0 mm, in the range of fuel temperature: 25–600 °C at near-critical pressures. In the single phase liquid flow, considerable free convection in laminar flow stabilizes the flow at Reynolds number (*Re*) up to 3600, the heat transfer coefficients can be predicted by Gnielinski correlation with deviations no more than 20.0% at $Re > 4000$; the adiabatic friction factor well agrees with the Moody diagram and Blasius correlation at laminar and turbulent flow respectively. As fuel temperature approaches the pseudo-critical point, peak and trough in heat transfer coefficients are recorded. First, heat transfer is enhanced by the boiling or pseudo-boiling at the relevant pressures. As fuel temperature increases, heat transfer deterioration takes place, accompanied with acoustic flow instability and peculiarly diabatic pressure drop deduction due to the steep thermodynamic properties. The heat transfer and flow stability are regained as the bulk fuel temperature increases to above the pseudo-critical points. Upon increasing the pressure, the singularities of heat transfer and fluid flow gradually disappear.

1. Introduction

The regenerative cooling technology is widely applied in heat protection of rocket engines [1,2] and scramjets [3,4] by using hydrocarbon fuel as coolant. Before injected into the combustion chamber as propellant, hydrocarbon fuel passes through the cooling passages (hydraulic diameter of about 1.0 mm) distributed in the hot wall of combustor. Large amounts of excess heat load are taken away for heat management purposes. In designing a fuel system for highly heated fuel, the identifications of fuel flow regimes, heat transfer and flow dynamic analysis in minichannel are the important aspects that need to be fully addressed.

In the open literature [5] for hydrocarbon fuel, the thermal instability and coke deposition were mainly focused on. But few attentions were paid to the fluid flow and heat transfer characteristics. Previous investigations on heat transfer of hydrocarbon fuel were mainly attributed to the active cooling of hydrocarbon/liquid oxygen rocket engines [1]. However, there are great distinctions between the regenerative cooling of scramjet and liquid rocket engine.

At Mach. 8 scramjet, the fuel temperature achieves 750 °C to provide a heat sink of 3.5 MJ kg^{-1} [3]. For rocket engine, the coolant temperature would not exceed the pseudo-critical point due to the huge amounts of fuel employed. As a result the single phase liquid flow occurs in the rocket, but the hydrocarbon fuel experiences boiling and multiphase flow in the scramjet. In summary the

Abbreviations: HTE, heat transfer enhancement; HTD, heat transfer deterioration.

* Corresponding author. Tel./fax: +86 (0)29 82665287.
E-mail addresses: qcbi@sohu.com, qcbi@mail.xjtu.edu.cn (Q. Bi).

1359-4311/$ – see front matter © 2012 Elsevier Ltd. All rights reserved.
http://dx.doi.org/10.1016/j.applthermaleng.2012.10.029

Nomenclature

D	inside diameter, mm
G	mass flux, kg m^{-2} s^{-1}
h	heat transfer coefficient, kW m^{-2} °C^{-1}
L_h	heated length, mm
L_f	length of the adiabatic channel, mm
P	pressure, MPa
q	heat flux, kW m^{-2}
T	temperature, °C
ΔP_h	diabatic pressure drop, kPa
ΔP_f	adiabatic pressure drop, kPa
Re	Reynolds number, $Re = GD/\mu$
Gr	Grashof number
Pr	Prandtl number

Greek letters

λ	friction factor
ρ	density of hydrocarbon fuel, kg m^{-3}
μ	viscosity of hydrocarbon fuel, Pa s

Subscripts

b	bulk fuel
w	wall
cr	critical
pc	pseudo-critical
sat	saturation

investigation on heat transfer of hydrocarbon fuel is filled with challenge and confusion due to the complicated fluid flow and heat transfer occurring in the cooling passage of scramjet.

Experiments were conducted by W.S. Hines [6] under the conditions wherein the vibration occurred, the fluid was at supercritical pressure, the wall temperature was greater than the critical temperature, and the bulk fuel temperature was considerable below critical temperature. Heat transfer with pseudo-boiling at $P > P_{cr}$ and surface boiling at $P < P_{cr}$ are always accompanied by pressure oscillations [7]. The flow instability and heat transfer deterioration always occur in the critical region due to the steep thermodynamic properties [8,9]. I.L. Pioro and R.B. Duffey [10,11] reviewed the hydraulic resistance and heat transfer in supercritical fluids flowing inside channels, the behaviors near the critical and pseudo-critical points were especially concerned.

In general, the majority of experiments were conducted in circular channels using water as working fluid, and hydraulic resistance data are limitedly compared with heat transfer data at supercritical pressures.

In this paper the fluid flow and heat transfer characteristics of endothermal hydrocarbon fuel were experimentally investigated in the practical aircraft fuel system conditions. Fuel temperatures ranged up to above pseudo-critical points. The effects of heat flux and pressure on the heat transfer of hydrocarbon fuel in a single minichannel were researched. Some singularities of other fluids in literature [10,11] were found in hydrocarbon fuel at the pseudo-critical temperature region.

2. Experimental sections

The experimental apparatus has been described in detail previously by Z. Liu (2012) [12]. A nickel alloy GH3128 (China) electrically heated channel (heated length L_h: 810 mm; inside diameter D: 2.0 mm; wall thickness: 0.5 mm) was used as test section. The average roughness of channel inner surface (Ra) is about 0.8 μm, measured by 3D Measuring Laser Microscope. The test section was horizontally distributed, as shown in Fig. 1.

The fuel inlet and outlet temperatures were measured by type K sheathed thermocouples with outside diameter of 1.0 mm, which were submerged in fluid. The 17 thermocouples (TC) of type K with outside diameter of 0.2 mm were spot-welded on bottom surface of the channel to measure the wall temperature. Spaces between thermocouples are 50.0 mm, and the two thermocouples at both ends (TC1 and TC17) are 5.0 mm away from the electrodes. To avoid the effect of submerged thermocouple on the flow field, the pressure taps were set between the electrode and sheathed thermocouple.

An adiabatic (unheated) channel (length L_f: 300 mm; inside diameter D: 2.0 mm) was set after the heated channel. Both channels were coated with thermal insulation cotton on the outside to reduce heat losses, and also to guarantee the accuracy of wall temperature measurement. Both the adiabatic pressure drop and outlet fluid temperature were measured for the adiabatic channel.

The fuel was feed by a plunger pump to pass through test channel. A Coriolis mass flow meter at the inlet was used to measure the mass flow rate. The outlet pressure and pressure drop across the test section were measured by Rosemont 3051 transducers. All the measured data were put into the computer by Isolated Measurement Pods 3595 (IMP3595) data acquisition system with frequency of 1.5 Hz. And a National Instrument (NI) was also used to collect the data with higher frequency of 1000 Hz to record the dynamic response of the measured parameters.

3. Data reduction

3.1. Pressure drop

The diabatic and adiabatic pressure drop were measured for the heated and unheated channel respectively. For the heated channel, the measured pressure drop ΔP_1 includes the diabatic pressure drop ΔP_h, minor loss ΔP_{m1}, inlet unheated ΔP_{in} and outlet unheated ΔP_{out} pressure drop.

$$\Delta P_h = \Delta P_1 - \Delta P_{m1} - \Delta P_{in} - \Delta P_{out} \quad (1)$$

The diabatic pressure drop ΔP_h, as shown in Eq. (1), consists of frictional and acceleration pressure drop in the horizontal channel.

For the unheated channel, the measured pressure drop ΔP_2 includes adiabatic frictional pressure drop ΔP_f and minor loss ΔP_{m2}, as shown in Eq. (2).

$$\Delta P_f = \Delta P_2 - \Delta P_{m2} \quad (2)$$

The Darcy friction factor λ of the adiabatic channel can be obtained from the frictional pressure drop, as shown in Eq. (3).

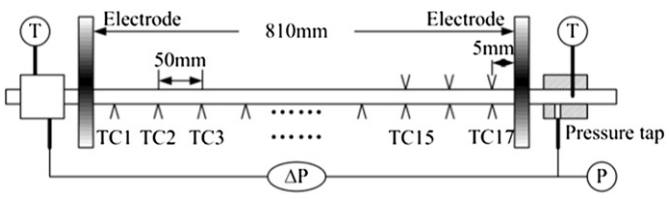

Fig. 1. The schematic figure of test section.

$$\lambda = \Delta P_f \frac{2\rho}{G^2}\frac{D}{L_f} \quad (3)$$

The Reynolds number is defined as $Re = GD/\mu_b$, where μ_b is the viscosity based on the bulk fuel temperature.

3.2. Heat transfer

Based on the last TC point on the heated channel, the local heat transfer coefficient h is determined by Eq. (4). The inside wall temperature T_w is determined by deducting the temperature drop through the measured outside wall temperature [13]. T_b is the bulk fuel temperature measured at the outlet. The heat flux q is determined from the measured voltage and current by deducting the heat loss, measured by the method of L. E. Faith [14].

$$h = q/(T_w - T_b) \quad (4)$$

The kerosene kind hydrocarbon fuel (provided by CNPC) is made up of a blend of hydrocarbons, with cycloalkanes 30.50 wt%, alkanes 20.06 wt% and aromatics 49.42 wt%, with average molecular formula of $C_{11.9}H_{23.4}$, and density of 838.0 kg m^{-3} at the condition of 25 °C and atmosphere pressure. The thermal physical properties of hydrocarbon fuel are mostly referred from Hu (1996) [15], which mainly include the viscosity and density at subcritical temperatures. There is little information available on the properties of hydrocarbon fuels at supercritical temperatures [5].

All the experimental uncertainties are summarized in Table 1. The uncertainties of λ and h would be no more than 2.8% and 4.0%, respectively.

4. Results and discussion

4.1. Pressure drop

4.1.1. The adiabatic pressure drop vs. fuel temperature

The adiabatic pressure drop vs. average fuel temperature is shown in Fig. 2 for different pressures. The average fuel temperature means the arithmetic average between inlet and outlet temperature. The temperature difference between inlet and outlet on the unheated channel would not exceed 20 °C, and the heat loss would be no more than 3.5%.

It can be seen that the pressure drop profiles with fuel temperature include two stages: (a) at fuel temperature below 400.0 °C, pressure change almost has no effect on adiabatic pressure drop, which is the characteristic of single phase liquid flow; (b) at fuel temperature above about 400.0 °C, pressure drop augments with pressure decreasing, which appears as a compressible fluid. The transition point at about 400 °C corresponds to the saturation temperature at subcritical pressure or the pseudo-critical temperature at supercritical pressure.

Table 1
Summary of the uncertainty analysis.

Parameters	Uncertainty
Diameter, D (%)	±1.0
Length, L (mm)	±1.0
Temperature, T (°C)	±0.5
Pressure drop, ΔP (kPa)	±0.25
Mass flux, G (%)	±1.2
Heat flux, q (%)	±2.3
Friction factor, λ (%)	±2.8
Reynolds number, Re (%)	±0.55
Heat transfer coefficient, h (%)	±4.0

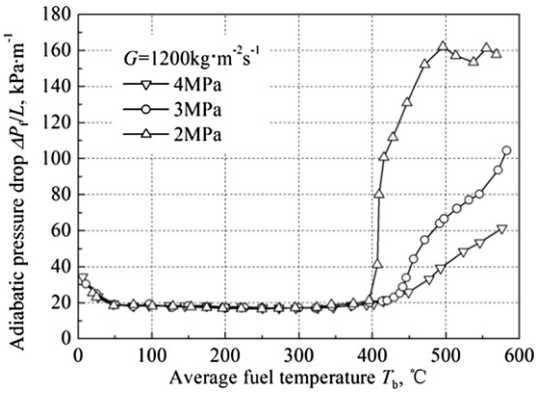

Fig. 2. The variation of adiabatic pressure drop with average fuel temperature of the unheated channel for different pressures.

In the first stage, the pressure drop decreases with the increasing fuel temperature from ambient to 50 °C, and then almost keeps no change at fuel temperature up to about 400 °C, which will be analyzed in the following part in details.

4.1.2. The adiabatic friction factor

The friction factors of unheated channel are analyzed for the single phase liquid flow ($T_b < 250$ °C). The analysis of pressure drops at higher fuel temperature is limited, for there are no available fuel properties at those conditions.

The variation of adiabatic pressure drops with Re are shown in Fig. 3 for different pressures ($P = 2, 3, 4$ MPa) and different mass fluxes ($G = 600, 900, 1200$ kg m^{-2} s^{-1}). At a given mass flux, different Reynolds numbers denote different average fuel temperatures of the unheated channel. The pressure drops are separated to three groups by the mass flux: larger pressure drop occurs at higher mass flux. The variations of pressure almost have no influence on the adiabatic pressure drop.

The variation of friction factors with Re at different fuel temperatures are shown in Fig. 4. Comparison of the experimental results with conventional correlations was conducted. Excellent agreement was obtained between experimental data and the predictive values by Blasius equation ($\lambda = 0.3164/Re^{0.25}$) at $Re > 2500$. And at $Re < 2000$ the laminar friction factors are identical with Moody diagram ($\lambda = 64/Re$). The transition Re was about 2000, consistent with that of the conventional channel.

In summary, the adiabatic friction factor is a function of Re. According to Eq. (3), at a given channel and mass flux, the frictional pressure drop correlates with fuel viscosity and density.

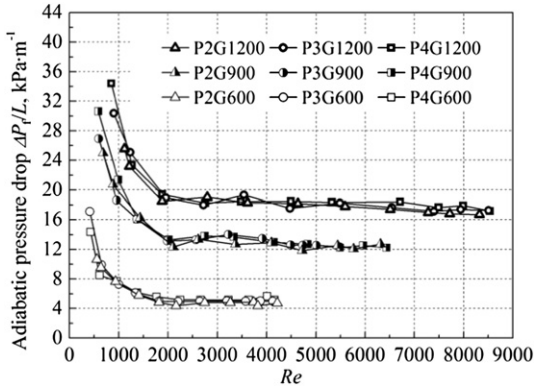

Fig. 3. The variation of adiabatic pressure drop with Re for different pressures and mass fluxes at fuel temperatures below 250 °C.

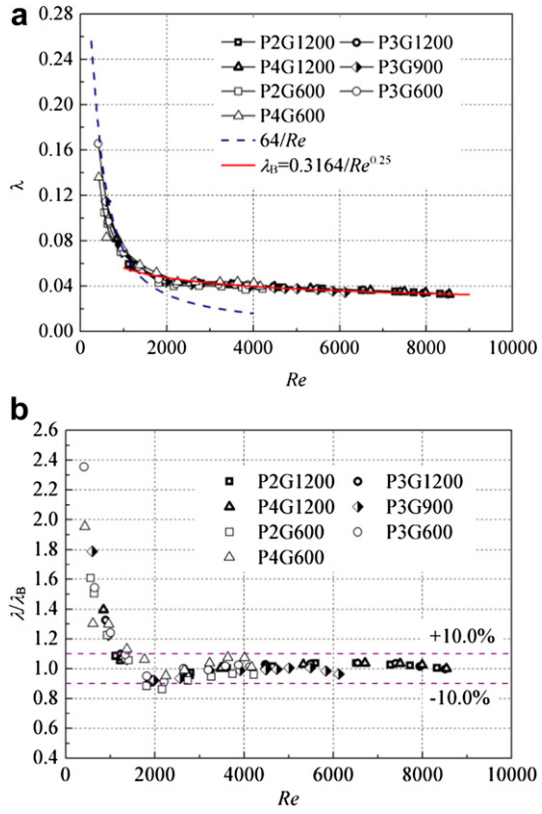

Fig. 4. Comparison of the measured friction factor with Blasius correlation for the unheated channel.

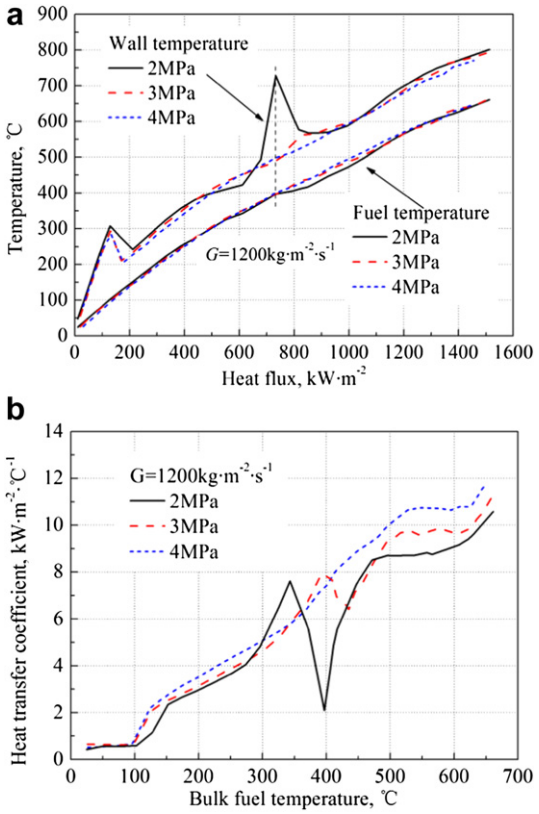

Fig. 5. Heat transfer behaviors at fuel temperature up to 600 °C for different pressures. (a) The local wall and fuel temperature and (b) heat transfer coefficients at the last TC point are shown.

At *Re* below 2000 the decreasing viscosity is the dominating factor, which results that the frictional pressure drop decreases with the increasing fuel temperature. However, the competitive effect of viscosity and density of hydrocarbon fuel nearly cancels out at fuel transition to turbulent flow, which results that the frictional pressure drops almost keep non-change with the increasing fuel temperature at single phase liquid flow.

4.2. Heat transfer

The heat transfer behavior of hydrocarbon fuel at fuel temperature up to 600 °C is shown in Fig. 5 for different pressures. In general, the wall and fuel temperature increase with the increasing heat flux, and the temperature differences between wall and fuel almost maintain at about 100 °C in the whole heat flux range. However, there are two special regions that the profiles of wall temperature and heat transfer coefficient are distinctive.

At low heat flux region, the wall temperature suddenly decreases and heat transfer coefficient increases quickly at $T_b \approx 100$ °C. It is caused by flow transition to turbulence as fuel temperature increases. It can be seen that the heat transfer coefficients are nearly constant at $T_b < 100$ °C at laminar flow.

The second special region is the large specific region, which is near the saturation point at subcritical pressure or the pseudo-critical point at supercritical pressure. Effect of pressure on heat transfer becomes significant in the region. The critical pressure and critical temperature of hydrocarbon fuel are about 2.5 MPa and 400 °C respectively, which are consistent with the critical properties of general kerosene hydrocarbons in the previous review by Edwards (1993) [16]. The singularities of heat transfer near pseudo-critical region is suppressed by the increasing pressure and disappears at $P = 4$ MPa.

Both the two special heat transfer regions will be analyzed in the following parts in details.

4.2.1. Turbulent heat transfer for single phase liquid flow

The variations of heat transfer coefficient with local bulk fuel temperatures and *Re* are shown in Fig. 6 at the condition of $T_w < T_{pc}$ wherein single phase liquid flow occurs ($T_b < 300$ °C, $T_w < 400$ °C). The curves of heat transfer coefficient vs. fuel temperature are divided into two groups by fuel mass flux G600 and G1200 at different pressures. The two groups merge into one curve while the dimensionless number *Re* is considered as horizontal ordinate. It indicates that the heat transfer coefficient at single phase liquid flow is a function of *Re*, which is affected by fuel temperature and mass flow rate but hardly by pressure.

It can be seen that the heat transfer coefficient slowly increases with the increasing *Re* at $Re < 3600$, which is a characteristic of laminar flow; The heat transfer coefficient deviates from the original trends to increase quickly at $3600 < Re < 4500$, which belongs to transition flow; and the heat transfer coefficient increased more quickly than that of laminar flow at $Re > 4500$ wherein the turbulent heat transfer occurs.

Comparison of the turbulent heat transfer data with empirical correlations is performed. The rewritten Dittus–Boelter (D–B) correlation [17] shown in Eq. (5) is applied to fluid flow in the range of *Re*: 10^4–1.2×10^5. Due to the lager temperature difference of about 100 °C between wall and fluid, the correlation modificated by viscosity is used.

$$h = 0.023 Re_b^{0.8} Pr_f^{0.4} \left(\frac{\mu_b}{\mu_w}\right)^{0.11} \frac{\lambda_b}{D} \tag{5}$$

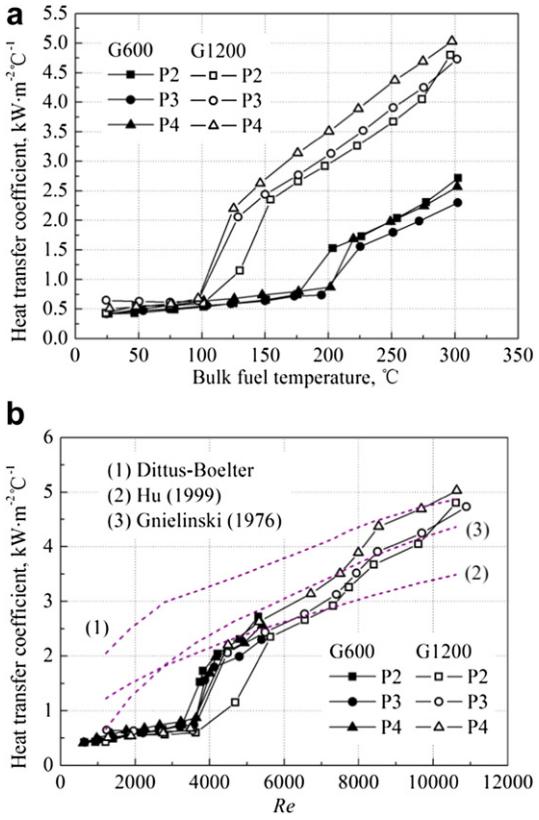

Fig. 6. The variation of heat transfer coefficient with (a) bulk fuel temperature and (b) *Re* for different pressures and mass fluxes at single phase liquid flow. All the curves calculated from existing correlations are based on the condition of P2G1200.

The Gnielinski [18] correlation shown in Eq. (6) is used in more widely range of *Re*: 2300–10^6.

$$h = 0.012(Re_b^{0.87} - 280)\, Pr_b^{0.4}\left[1 + \left(\frac{D}{L}\right)^{2/3}\right]\left(\frac{Pr_b}{Pr_w}\right)^{0.11}\frac{\lambda_b}{D} \quad (6)$$

Hu [19] experimentally investigated the heat transfer of kerosene kind hydrocarbon fuel at the condition of $T_w < T_{pc}$, and a correlation shown in Eq. (7) was fitted with uncertainties of 10.0%. The diameter of test channel was 1.7 mm and the mass flow rate ranged of 5000–40,000 kg m^{-2} s^{-1}, which is applied to the rocket regenerative cooling.

$$h = 0.008Re_b^{0.873}Pr_b^{0.451}(\lambda_b/D) \quad (7)$$

Results indicated that the turbulent heat transfer coefficients are always between the predicated curve of Hu and D–B correlation. And the Gnielinski correlation agrees best with the experimental data. Comparison of the experimental data with predictive value by Gnielinski correlation at $Re > 4000$ is presented in Fig. 7 with uncertainties no more than 20.0%, RMS = 12.0%.

It is noticed that the transition flow begins at $Re \approx 3600$, which is much larger than the value of 2000 obtained at the adiabatic channel above. That the transition *Re* increased is a result of considerable free convection occurred at laminar flow in the heated channel. As the fuel was heated, the temperature differences between the top and bottom of the channels were motivated by free convection imposed on the laminar flow [14]. The heated fuel at the wall with less density rose in the boundary layer from the

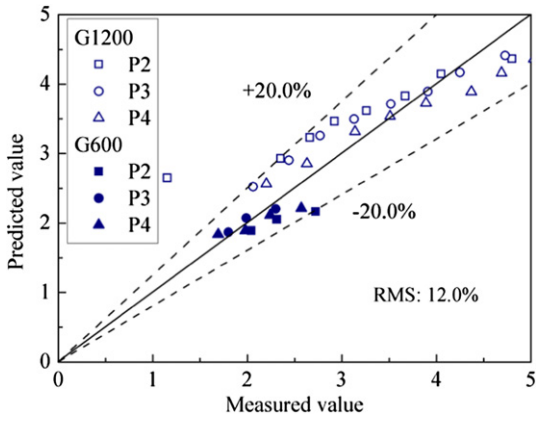

Fig. 7. Comparison of the measured heat transfer coefficient with the predicted one by Gnielinski (1976) [18] correlation, RMS is 12.0%.

bottom to the top of the channel, thus causing the top of the channel to become hotter than the bottom. And the bottom of the channel was cooled by the colder fluid circulating down from the core of the fluid.

The laminar flow can be apparently stabilized by free convection, which can be indicated by the increased limit on the Reynolds number for laminar flow at high Grashof numbers. The modified Grashof number [14] based on the difference in densities at the bulk fluid and wall temperatures is show in Eq. (8), where *g* is the acceleration of gravity.

$$Gr = \frac{gD^3\rho_b(\rho_b - \rho_w)}{\mu_b^2} \quad (8)$$

Reports of L.E. Faith [14] showed that laminar flow at the condition with $Gr > 10^5$ occurred at all Reynolds number below 5000. However, at conditions with $Gr < 10^4$ laminar flow only occurred at Reynolds number below 2300, using hydrocarbon fuel as working fluid.

The temperature differences between the top and bottom of the channels for different operating conditions are shown in Fig. 8 as a function of *Re*. The maximum values of temperature differences were recorded at average *Re* of 3578, and $Gr = 8.6 \times 10^4$ at P3G600 condition. Results indicated that the free convection stabilized the laminar flow at *Re* up to 3578 for high Grashof numbers, at laminar flow the temperature differences increased with *Re*, and the turbulent flow caused that the temperature difference suddenly

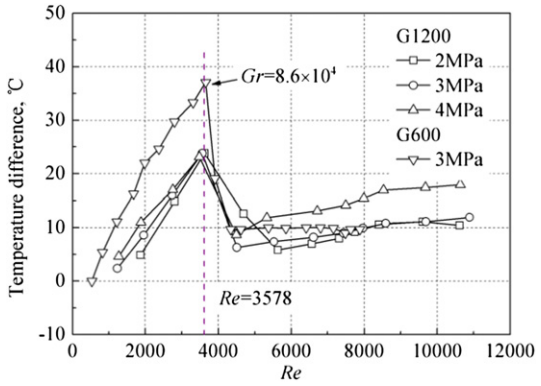

Fig. 8. Temperature differences between the top and bottom of channel with *Re* at the last TC point.

decreased at $Re = 3578$, which was consistent with the heat transfer enhancement at $Re \approx 3600$, as shown in Fig. 6(b).

4.2.2. Heat transfer near pseudo-critical temperature

Heat transfer coefficient varies strongly near the pseudo-critical point due to the steep thermal physics properties [8]. All the normally, deteriorated and improved heat transfer appear near the critical or pseudo-critical points. A peak in heat transfer coefficient near the pseudo-critical point was recorded [11]. The operating conditions also affected the heat transfer, such as the heat flux, mass flux and pressure.

In our paper, peak and trough in heat transfer coefficients near the boiling or pseudo-boiling region are recorded at $T_b = 300–500$ °C, as shown in Fig. 5(b). Following the heat transfer enhancement (HTE), heat transfer deterioration (HTD) happens, and then the heat transfer is suddenly enhanced again with the increasing fuel temperature.

The first HTE starts at the condition of $T_b = 273.2$ °C, $T_w = 381.0$ °C at $P = 2$ MPa wherein the fuel saturation temperature $T_{sat} = 387.0$ °C. HTE was always obtained at low heat fluxes as the bulk fluid temperature approached the saturation point or pseudo-critical point [8], which was a result of the occurrence of subcooled boiling or pseudo-boiling at the relevant pressures.

As the fuel density rapidly decreases during the evaporating process, the HTD takes place at higher fuel temperature. The maximum heat transfer coefficient achieves and the HTD begins at the condition of $T_b = 343.0$ °C, $T_w = 423.0$ °C wherein the film temperature $T_f = 383.0$ °C ($T_f = (T_b + T_w)/2$), near the saturation point ($T_{sat} = 387.0$ °C). X. Cheng [8] summarized in his review that the HTD was only observed in the following temperature condition: $T_b < T_{pc} < T_w$, which was also consistent with the result of this presentation. That the peak of heat transfer coefficient recorded at film temperature near the pseudo-critical point was seen in previous literature of Swenson et al. [20].

Some researchers [21,22] suggested that the maximum heat transfer coefficient corresponded to a bulk fluid enthalpy, which was slightly less than the pseudo-critical enthalpy. And the peak in heat transfer coefficient was a result of the variation in thermal properties near the pseudo-critical point. The deteriorated heat transfer regime always appeared together with the improved heat transfer regime, which is also seen in the results of Fig. 5 at $P = 2.0$, 3.0 MPa. And the improved heat transfer is eventually replaced with the deteriorated heat transfer as heat flux increases.

Fig. 9 shows that the second HTE begins at $T_b = 440$ °C at the condition of P3G1200, which is accompanied with diabatic and adiabatic pressure drop increasing rapidly. It indicates that the fuel temperature of about 440 °C is the pseudo-critical point at $P = 3$ MPa, and the steep thermodynamic properties especially the rapidly decreasing density result that the pressure drops increase quickly.

The pressure drop and heat transfer characteristics divided into three stages are clearly shown in Fig. 9 at supercritical pressure of 3.0 MPa. The first HTE is caused by pseudo-boiling at the condition of T_b (300–374.2 °C) $< T_{pc}$, which results that the diabatic pressure drop increases faster than adiabatic pressure drop with the increasing fuel temperature. The evaporative liquid is condensed in the bulk fluid, which prevents the adiabatic pressure drop increasing rapidly.

The HTD at the condition of P3G1200 happens at $T_b = 400–440$ °C wherein the adiabatic pressure drop increases faster than before. Great attention is paid to the diabatic pressure drop, which decreases in this stage. The singularity of the pressure drop characteristic in the heated channel was also found in the previous literature [23,24] in the pseudo-critical region. The pressure drop deduction will be analyzed in the following part in detail.

4.2.3. The flow instability accompanied with boiling or pseudo-boiling

As fuel temperature increases, the diabatic pressure drop decreases near the pseudo-critical point. It is noticed that the phenomena is strongly relevant to the fluid flow instability accompanied with cyclical acoustic vibration. The observed pressure drop deduction, flow instability and HTD happen simultaneously at operating condition of P3G900, as shown in Figs. 10 and 11.

The fluid flow maintains stably at $T_b < 400$ °C, and then flow instability suddenly happens with the increasing heat flux. The stability could not be regained while the heat flux was designedly

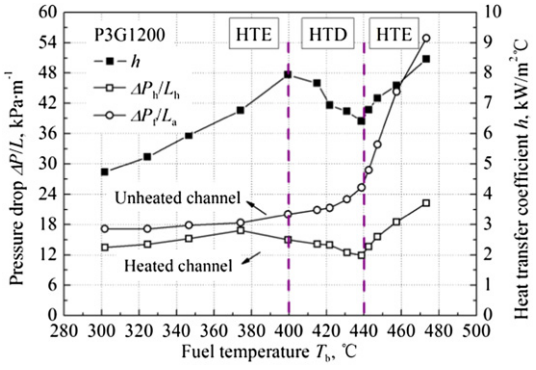

Fig. 9. The pressure drop and heat transfer behaviors in the critical region at P3G1200 condition. The horizontal ordinate is fuel outlet temperature for ΔP_h and average fuel temperature for ΔP_f.

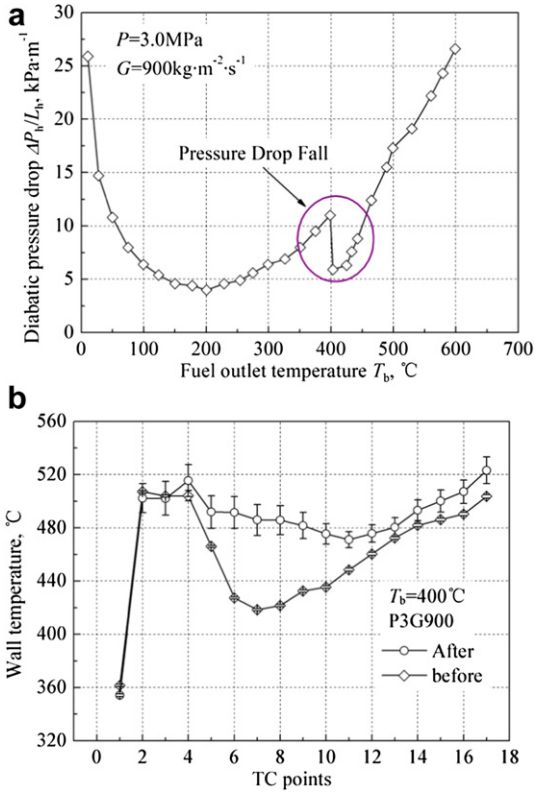

Fig. 10. (a) The diabatic pressure drop and (b) heat transfer behavior of hydrocarbon fuel before and after oscillation occurs at the condition of P3G900.

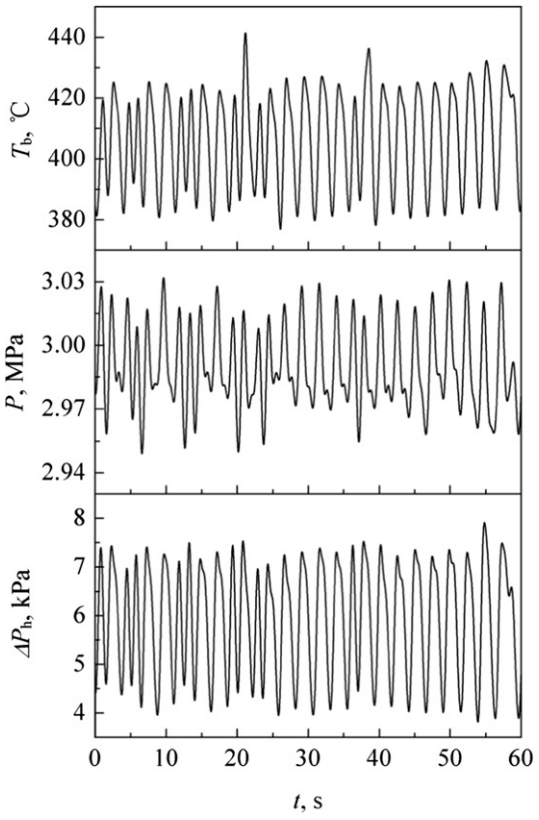

Fig. 11. The instability curves of fuel outlet temperature, pressure and diabatic pressure drop at the condition of P3G900. Average T_b = 402.8 °C, P = 2.99 MPa, ΔP_h = 5.9 kPa. Amplitude of oscillation: T_b-41.2 °C, 10.2%; P-0.054 MPa, 1.8%; ΔP_h-3.1 kPa, 52.5%.

reduced to the value of original stable condition. Fig. 10(a) shows that the diabatic pressure drop suddenly decreases (Pressure Drop Fall) while the instability takes place at $T_b \approx 400$ °C. Fig. 10(b) shows the wall temperature profiles along the channel at the condition of $T_b \approx 400$ °C before and after the oscillation occurred. Results show that the wall temperatures increase obviously and HTD happens after the onset of oscillation.

Fig. 11 shows the flow instability curves at fuel outlet temperature T_b = 402.8 °C. The fuel outlet temperature, pressure and diabatic pressure drop fluctuate in phase with period of about 2.0 s. The audible instabilities have been noted in previous literature [6,25,26] with supercritical hydrocarbon fuel, and explanations of the cause have been proposed. But in contradictory result, the audible instability was corresponded to a significant enhancement in heat transfer [25], and the pressure drop characteristic was not analyzed. In the recent research by J. Barber [27,28], the bubble dynamics of flow boiling which led to the pressure and temperature fluctuation were carefully analyzed. The bubble expansion instability is similar to the phenomena here. The frequency of the instability is driven by the bubble dynamics and the channel wall thermal properties.

The instability region at the condition of P3G1200 is shown in Fig. 12. The uncertainties of fuel outlet temperature T_b, diabatic pressure drop ΔP_h and adiabatic pressure drop ΔP_f are presented. Results show that the instabilities occur with bigger uncertainties at fuel temperature range of 360–440 °C than other temperatures, which is accordance with the region of diabatic pressure drop deduction and HTD.

The flow instability regime of hydrocarbon fuel is complicated and the instability region will be affected by operating

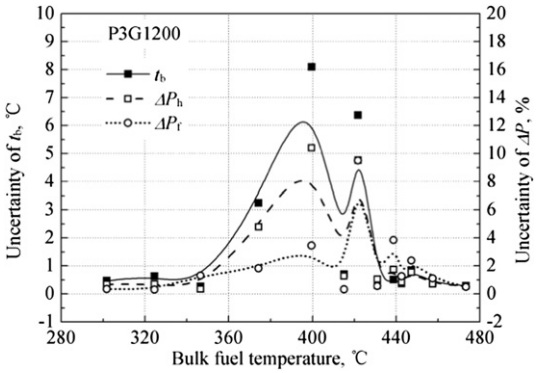

Fig. 12. Instabilities at the pseudo-critical region. t_b is fuel outlet temperature of heated channel. Uncertainties are calculated as 1.962 × σ (Standard deviation).

conditions, such as pressure, mass flow rate, heat flux, and channel diameter and heated length and so on. Diane L. Linne [26] experimentally investigated the instabilities of hydrocarbon fuel at supercritical pressures in details and found that it was profoundly difficult to uncover the regime and onset of instabilities. However, the HTE and HTD at instability condition agree with the result reported.

The instabilities, pressure drop deduction, and HTD can happen simultaneously or in turn. Fig. 10 shows that the three incidents happen simultaneously at $T_b \approx 400$ °C at the condition of P3G900. And at the condition of P3G1200 the instabilities begin at 345 °C, and pressure drop deduction begins at 374.2 °C, and HTD begins at 400 °C, as seen in Figs. 9 and 11. It is still unknown that how the fluid instabilities are triggered. However, it can be sure that it happens at higher fuel temperature if the three incidents happen simultaneously like that at the condition of P3G900.

In summary, the flow instabilities take place at the conditions of $T_b < T_{pc} < T_w$ and the stably can be regained while $T_b > T_{pc}$. The two-phase flow boiling at subcritical pressure or pseudo-boiling at supercritical pressure caused the flow instability. While the fluid is far away from the critical region with $T_b > T_{pc}$ or $T_b > T_{sat}$, the fluid flow regains stable like the single phase gas flow.

5. Conclusion

The convective heat transfer and pressure drop characteristics of a kerosene kind hydrocarbon fuel were experimentally investigated in an electrically heated channel at fuel temperature up to points above the critical region at near-critical pressures. The heat transfer and its interaction with pressure drop were analyzed at wall temperature below and above the pseudo-critical point respectively. It concluded that:

(1) The adiabatic friction factors at single phase liquid flow agree well with the conventional Moody diagram at laminar low and Blasius correlation at turbulent flow. The larger diabatic pressure drop would be produced at lower pressure while boiling or pseudo-boiling occurred at the relevant pressures. The pressure drop would increase rapidly at fuel temperature of above pseudo-critical points.
(2) It experienced single phase liquid flow laminar and turbulent heat transfer, and flow boiling heat transfer enhancement and deterioration in the critical region at subcritical pressures. The considerable free convection stabilized the laminar flow at Re up to 3600 at high Grashof numbers. The heat transfer coefficients well agree with Gnielinski correlation with deviations no more than 20.0% at $Re > 4000$ in the single phase liquid flow.

(3) Peak and trough in heat transfer coefficients near the pseudo-critical point were recorded. The pseudo-boiling heat transfer enhancement occurred at fuel temperature below and wall temperature above pseudo-critical point at supercritical pressure. Heat transfer deterioration would take place as film temperature approached the pseudo-critical point, accompanied with acoustic flow instability and diabatic pressure drop deduction in the critical region. At the condition of $T_b > T_{pc}$, heat transfer and flow stability would be regained. The singularities would be reduced and disappeared with the increasing pressure.

The heat transfer and pressure drop in the critical region are still an elusive problem. Many peculiarly phenomena would occur due to the steep thermodynamic properties. The effects of heat flux, mass flux and channel diameter on the special characteristic in the critical region are needed to be investigated continuously and carefully.

References

[1] R.W. Bates, T. Edwards, Heat Transfer and Deposition Behavior of Hydrocarbon Rocket Fuels, AIAA 2003-123.
[2] M.C. Billingsley, Thermal Stability and Heat Transfer Characteristics of RP-2, AIAA 2008-5126.
[3] T. Edwards, Liquid Fuels and Propellants for Aerospace Propulsion (1903) (2003). AIAA 2003–6946.
[4] J.M. Reddecliff, J.W. Weber, Development and Demonstration of a Hydrocarbon Scramjet Propulsion System, AIAA 1998-1613.
[5] T. Edwards, USAF Supercritical Hydrocarbon Fuels Interests, AIAA 93–0807.
[6] W.S. Hines, H. Wolf, Pressure oscillations associated with heat transfer to hydrocarbon fluids at supercritical pressures and temperatures, ARS J. (1962) 361–366.
[7] N.L. Kafengauz, M.I. Fedorov, Pseudoboiling and heat transfer in a turbulent flow, J. Eng. Phys. Thermophys. 14 (5) (1968) 489–490.
[8] X. Cheng, T. Schulenberg, Heat Transfer at Supercritical Pressures: Literature Review and Application to an HPLWR, FZKA6609 (2001).
[9] Y.Y. Hsu, J.M. Smith, The effect of density variation on heat transfer in the critical region, J. Heat Transfer 83 (2) (1961) 176–181.
[10] I.L. Pioro, R.B. Duffey, et al., Hydraulic resistance of fluids flowing in channels at supercritical pressures (survey), Nucl. Eng. Des. 231 (2) (2004) 187–197.
[11] I.L. Pioro, R.B. Duffey, Experimental heat transfer in supercritical water flowing inside channels (survey), Nucl. Eng. Des. 235 (22) (2005) 2407–2430.
[12] Z. Liu, Q. Bi, Y. Guo, et al., Heat transfer characteristics during subcooled flow boiling of a kerosene kind hydrocarbon fuel in a 1 mm diameter channel, Int. J. Heat Mass Transfer 55 (2012) 4987–4995.
[13] J.R.S. Thom, W.M. Walker, et al., Boiling in subcooled water during flow up heated tubes or annuli, Proc. Inst. Mech. Eng. 180 (1966) 226–246.
[14] L.E. Faith, G.H. Ackerman, H.T. Henderson, Heat Sink Capabilities of Jet A Fuel: Heat Transfer and Coking Studies, NASA CR-72951 (July 1971).
[15] Z.H. Hu, Experimental Investigation on Heat Transfer Characteristics of Kerosene Used in Rocket Engine, Master's thesis, Xi'an Jiaotong University, Xi'an, 1996.
[16] T. Edwards, S. Zabarnick, Supercritical fuel deposition mechanisms, Ind. Eng. Chem. Res. 32 (12) (1993) 3117–3122.
[17] F.W. Dittus, L.M.K. Boelter, Heat Transfer in Automobile Radiators of the Tubular Type, vol. 2, Publications on Engineering, University of California, Berkeley, 1930, pp. 443.
[18] V. Gnielinski, New equation for heat and mass transfer in turbulent pipe and channel flow, Intern. Chem. Eng. 16 (2) (1976) 359–366.
[19] Z.H. Hu, T.K. Chen, Y.S. Luo, et al., Heat transfer characteristics of kerosene at supercritical pressure, J. Xi'an Jiaotong Univ. 9 (33) (1999) 62–65.
[20] H.S. Swenson, J.R. Carver, et al., Heat transfer to supercritical water in smooth-bore tubes, J. Heat Transfer 87 (4) (1965) 477–483.
[21] K. Yamagata, K. Nishikawa, S. Hasegawa, et al., Forced convective heat transfer to supercritical water flowing in tubes, Int. J. Heat Mass Transfer 15 (12) (1972) 2575–2593.
[22] M.A. Styrikovich, T.K. Margulova, Z.L. Miropol'skii, Problems in the development of designs of supercritical boilers, Therm. Eng. 14 (6) (1967) 5–9.
[23] N.S. Kondrat'ev, Heat transfer and hydraulic resistance with supercritical water flowing in tubes, Therm. Eng. 16 (8) (1969) 73–77.
[24] N.V. Tarasova, A.I. Leont'ev, Hydraulic resistance during flow of water in heated pipes at supercritical pressures, High Temp. 6 (4) (1968) 721–722.
[25] D.L. Linne, M.L. Meyer, T. Edwards, D.A. Eitman, Evaluation of Heat Transfer and Thermal Stability of Supercritical JP-7 Fuel, AIAA 1997-3041.
[26] D.L. Linne, et al., Investigation of Instabilities and Heat Transfer Phenomena in Supercritical Fuels at High Heat Flux and Temperatures, AIAA 2000-3128.
[27] J. Barber, D. Brutin, K. Sefiane, et al., Bubble confinement in flow boiling of FC-72 in a "rectangular" microchannel of high aspect ratio, Exp. Therm. Fluid Sci. 34 (8) (2010) 1375–1388.
[28] J. Barber, D. Brutin, K. Sefiane, et al., Unsteady-state fluctuations analysis during bubble growth in a "rectangular" microchannel, Int. J. Heat Mass Transfer 54 (23–24) (2011) 4784–4795.